Faraday Discussions

RSC Publishing

Cite this: *Faraday Discuss.*, 2013, **164**, 283

PAPER

Highly sensitive detection of nitroaromatic explosives at discrete nanowire arrays

Sean Barry,[a] Karen Dawson,[a] Elon Correa,[b] Royston Goodacre[b] and Alan O'Riordan*[a]

Received 4th March 2013, Accepted 18th April 2013

DOI: 10.1039/c3fd00027c

We show a photolithography technique that permits gold nanowire array electrodes to be routinely fabricated at reasonable cost. Nanowire electrode arrays offer the potential for enhancements in electroanalysis such as increased signal-to-noise ratio and increased sensitivity while also allowing quantitative detection at much lower concentrations. We explore application of nanowire array electrodes to the detection of different nitroaromatic species. Characteristic reduction peaks of nitro groups are not observed at nanowire array electrodes using sweep voltammetric methods. By contrast, clear and well-defined reduction peaks are resolved using potential step square wave voltammetry. A Principle Component Analysis technique is employed to discriminate between nitroaromatic species including structural isomers of DNT. The analysis indicates that all compounds are successfully discriminated by unsupervised cluster analysis. Finally, the magnitude of the reduction peak at −671 mV for different concentrations of TNT exhibited excellent linearity with increasing concentrations enabling sub-150 ng mL^{-1} limits of detection.

1 Introduction

The dual-use molecule, 2,4,6-trinitrotoluene (TNT), and its analogues, is used within the bulk chemical industry for the manufacture of dyes, plasticisers, herbicides, *etc.* while it is also employed as ammunition and an explosive for military applications.[1] TNT is highly soluble in water (~150 mg L^{-1})[2] and its presence in waste and ground water is an on-going concern for environmental, health and security reasons. TNT is highly toxic and has been linked with anaemia, skin irritation, and abnormal liver function in humans.[3,4] Based on animal studies, the US Environmental Protection Agency (EPA) has recently identified TNT as a potential human carcinogen as both TNT and its metabolites are toxic and genotoxic at relatively low concentrations, *i.e.*, at

[a]*Tyndall National Institute – University College Cork, Lee Maltings, Dyke Parade, Cork, Ireland. E-mail: alan.oriordan@tyndall.ie; Tel: +353 21 2346403*

[b]*School of Chemistry, Manchester Institute of Biotechnology, University of Manchester, 131 Princess Street, Manchester, M1 7DN, UK*

levels above 2 μg mL^{-1}.[5] As a result, the EPA has issued health advisories concerning its maximum allowable levels in potable and ambient waters.

Field analyses for environmental monitoring have shown the need for portable, easy-to-use, low maintenance and sensitive methods to enable rapid detection and quantification of these contaminants of interest at reasonable economic cost. A further impetus in this regard is on-going security concerns and the need to develop approaches for remote and decentralised security screening. A variety of techniques including enhanced Raman,[6] UV absorption,[7] surface plasmon resonance[8] and fluorescence[9] spectroscopies, enzyme linked immunosorbent assays,[10] solid/liquid phase extraction (pre-concentration) followed with GC- or HPLC- mass spectrometry[11–13] are commonly employed for the detection of TNT and its analogues. While all of these approaches can quantitatively detect nitroaromatic species within the detection range of 0.01–5000 ng ml^{-1}, the associated instruments are complex, have a high cost of ownership and are not ideally suited to field analysis.

Recent advances in nanofabrication have enabled the development of a new range of highly sensitive nanosensors that are compact, low power, highly sensitive and have extremely small sample volume requirements. One-dimensional nanostructure based field effect transistors (FET) employing silicon,[14] carbon nanotubes,[15] III–V semiconductors,[16] conducting polymers[17] and metal oxide nanowires[18] are an emerging class of nanosensor finding application in label-free sensing. However, the sensing mechanisms of FET devices arise from perturbations of their local electrostatic environment by charged analyte species. As such, they are limited to the detection of large and highly charged species, such as biomolecules, and are mostly insensitive to small or uncharged molecules important in environmental/security monitoring.

Unlike FETs, noble metal nanowires such as gold, platinum and silver, are important because of their excellent electrical and optical properties. Gold nanowires are of particular interest due to their high chemical and thermal stability, and excellent electrical conductivity and have tremendous potential in electroanalysis. In electrochemistry, nanoelectrodes offer a number of enhancements compared to macroelectrodes due to their many advantageous properties: low background charging; high current density due to enhanced mass transport; low depletion of target molecules; low supporting electrolyte concentrations; and faster response times.[19,20,21] Recently, highly sensitive gold nanowire-based sensors for the electrochemical detection of small molecules including hydrogen peroxide,[22,23] dopamine,[24] and glucose[25] have been reported.

Nanoscale electroanalytical approaches are particularly suited for detection of nitroaromatic species due to the inherent redox activity of these molecules. The electroreduction pathways of the nitro groups in nitroaromatics have been well documented in the literature.[26] Firstly, a nitroso intermediate followed by a hydroxylamine intermediate are formed *via* a $4e^-/4H^+$ electron and proton transfer system. The hydroxylamine group is further reduced to an amine *via* a $2e^-/2H^+$ electron and proton transfer system, see Scheme 1. In acidic media, each nitro group in TNT is sequentially reduced to amino groups producing three peaks at increasing negative potentials at glassy carbon electrodes. As tri-nitro compounds, including TNT, may be more readily reduced at metallic electrodes compared to mono- or dinitro-compounds,[27] in this work we develop gold

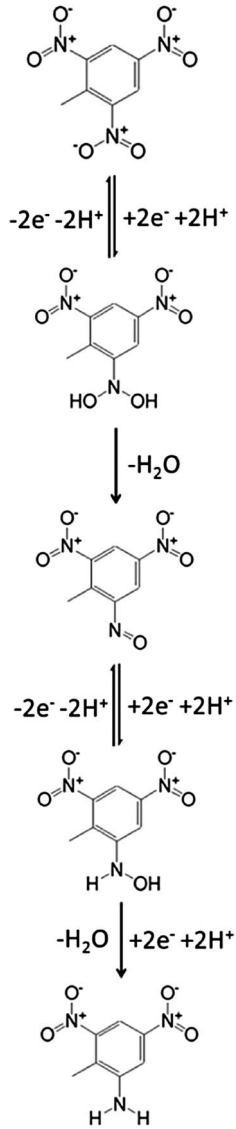

Scheme 1 Electrochemical reduction pathway of nitroaromatic species – 2,4,6-trinitrotoluene.

nanowire-based devices and explore their application to the sensitive detection of TNT and its analogues including nitrotoluene (NT), 2,4-dinitrotoluene (2,4-DNT), 2,6- dinitrotoluene (2,6-DNT) and 1,3-dinitrobenzene (1,3-DNB).

2 Experimental

Chemicals and materials

Sodium phosphate monobasic, sodium phosphate dibasic, 3-nitrotoluene (3-NT), 2,4-dinitrotoluene (2,4-DNT), 2,6-dinitrotoluene (2,6-DNT), 1,3-dinitrobenzene (1,3-DNB), 2,4,6-trinitrotoluene (TNT) and acetonitrile are purchased from

Sigma-Aldrich and used as received. A sample of military grade 2,4,6-trinitrotoluene is provided by the Ordnance School, Defence Forces Ireland. Deionized water (18.2 MΩ cm) from an ELGA Pure Lab Ultra system is used for the preparation of samples. All electrochemical measurements are undertaken in a 50 mM phosphate buffer solution (pH 6.5).

Electrode fabrication

Gold nanowire array electrodes, interconnection tracks, peripheral contact pads and two central micron scale half-disc microelectrodes are fabricated using a photolithography process on four inch wafer silicon substrates bearing a ~300 nm layer of thermally grown silicon dioxide (Si/SiO_2). In this process, metallic structures are patterned in a photoresist layer (Microposit LOR 10A, 500 nm) using an optical mask. Following resist development, gold layers (Ti/Au, 10/100 nm) are blanket deposited by metal evaporation (Temescal FC-2000 E-beam evaporator) and removed from un-patterned areas using standard lift-off techniques. A further metal deposition (Ti/Pt 10/90 nm) step is then performed onto one half-disk electrode. In this manner, one central half-disk electrode may be employed as a gold counter and the other as a platinum pseudo-reference electrode, respectively.

To prevent unwanted electrochemical reactions occurring between metal interconnection tracks and electrochemically active species, a silicon nitride passivation layer (~500 nm) is then deposited by plasma-enhanced chemical vapour deposition (PECVD) onto the wafer surface. Photolithography and dry etching are then employed to selectively open windows (~45 × 100 μm) in the passivation layer directly above the gold nanowire working electrodes to allow exclusive contact between them and an electrolytic solution. Openings are also maintained above the counter and reference electrodes, along with peripheral contact pads. Following fabrication, wafers are diced into 16 × 16 mm chips, such that each chip contains twelve individually contacted gold nanowire working electrode arrays, an integrated gold counter electrode and a platinum pseudo-reference electrode.

Optical and electrical characterisation

Optical micrographs of nanowire electrode arrays are acquired using a calibrated microscope (Axioskop II, Carl Zeiss Ltd.) equipped with a charge-coupled detector camera (CCD; DEI-750, Optronics). As a quality control check, to confirm electrical functionality, two-point electrical measurements are performed using a probe station (Model 6200, Micromanipulator Probe Station) in combination with a source meter (Keithly 2400) and a dedicated LabVIEW™ V8.0 program. In these current–voltage (*I–V*) measurements, the source electrode is grounded, a bias sweep up to ±10 mV is applied to the drain electrode, and the current through the nanowire is measured.

Electrochemical analysis

All electrochemical studies are performed using a CHI660a Electrochemical Analyzer and a Faraday Cage CHI200b (CH Instruments) connected to a PC. Experiments employ a standard three-electrode cell configuration using a gold nanowire arrays as the working electrodes *versus* the on-chip gold counter

electrode and on-chip platinum pseudo-reference electrode. A custom holder is employed comprising a 180 μL sample volume well and spring loaded gold pins to permit electrical contact to electrodes. Cyclic voltammetry experiments (CV) are conducted in 10 mM phosphate buffer saline (PBS, pH 7.4) containing 1 mM ferrocenemonocarboxylic acid (FcCOOH, Sigma Aldrich) in the voltage range of −0.15 V to 0.45, *versus* on-chip platinum pseudo-reference to first confirm electrochemical functionality. Stock solutions of 1000 μg mL^{-1} of 3-NT, 2,4-DNT, 2,6-DNT, 1,3-DNB and TNT (military sourced) are freshly prepared in acetonitrile prior to use. Analytical TNT standards (Spectroscopic grade) are also purchased pre-prepared in ampules as 1000 μg mL^{-1} in acetonitrile (Aldrich). Stock solutions are diluted using phosphate buffer as required. Typical measurements are performed using 100 μL of solution (covering all three electrodes) without stirring or purging of dissolved oxygen with nitrogen. Concerning calibration plots, serial additions are performed by adding 5 or 10 μL aliquots (of stock solution) as appropriate and mixed by agitating the solution using within the volume ranges of 95 μL to 180 μL. All experiments are performed at room temperature.

Cyclic voltammetry (CV) is conducted in 50 mM phosphate buffer solution (PB, pH 6.5) containing 50 μg mL^{-1} of the compound of interest in the voltage range of 0 V to −1.0 V, *versus* on-chip platinum pseudo-reference using a scan rate of 40 mV s^{-1}. A blank measurement (not shown) of PB only is also recorded. Square Wave Voltammetry (SWV) is performed by sweeping the potential from −0.4 V to −1.02 V for individual species. A scan range of −0.4 V to −0.97 V is employed for serial additions of TNT. The slightly longer scan range for the individual compounds is necessitated by the cathodic potential of the 3-NT reduction to ensure a complete peak is observed. All scans are performed using a frequency of 10 Hz, amplitude of 50 mV and a potential step of 4 mV. Blank SWV are also obtained for the purpose of background subtraction.

3 Results and discussion

Gold nanowire arrays are fabricated using a photo-lithography process at Si/SiO_2 substrates as described in the Experimental section. Each chip contains twelve different nanowire electrode arrays along with integrated gold counter and

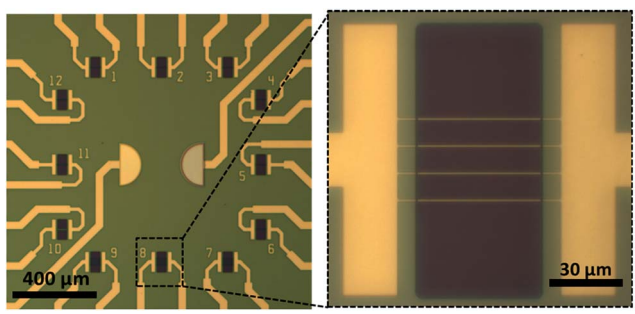

Fig. 1 (a) plan view of the central chip region which contains 12 individually addressable nanowire electrodes, a gold on-chip counter electrode (left) and a platinum on-chip pseudo reference electrode (right). (b) Higher magnification image of a nanowire array electrode comprising four nanowires.

platinum pseudo-reference electrodes and are structurally characterised using optical microscopy following fabrication. Fig. 1(a) shows an optical micrograph of the central chip region which contains the 12 individually addressable nanowire electrodes, along with the half-disc gold on-chip counter electrode (left) and platinum on-chip pseudo reference electrode (right). Fig. 1(b) optical image of a fully fabricated, integrated and passivated nanowire array device comprising four nanowires. The width of the passivation window (central dark rectangle) defines the exposed nanowire length at 45 μm. Standard two-point *I–V* measurements in air are undertaken as a quality control check to ensure that all nanowire electrodes are fully functional prior to electroanalysis. A voltage bias of ±10 mV is selected to confirm Ohmic behaviour. The low voltage range is chosen to avoid undesired electro-migration effects which may damage the nanowires. The electrical behaviour observed at fully fabricated single nanowires is very reproducible with all functioning nanowire array devices displaying linear Ohmic responses with low resistances (62 ± 4 Ω), see Fig. 2(a). This low variation (~6.4%) in electrical performance for discrete nanowire arrays is excellent and is consistent with that observed for nanowire dimensions. Control electrical measurements were obtained in the absence of nanowire arrays, yielding very high resistances (~10 GΩ) typical of an open circuit. This confirms that the underlying silicon oxide functioned as an effective insulating layer preventing electrical coupling with the silicon beneath and that the observed electrical characteristics were exclusively generated by the nanowire arrays. Nanowire array devices that exhibit high resistances or open circuits are discarded and not used for electrochemical analysis.

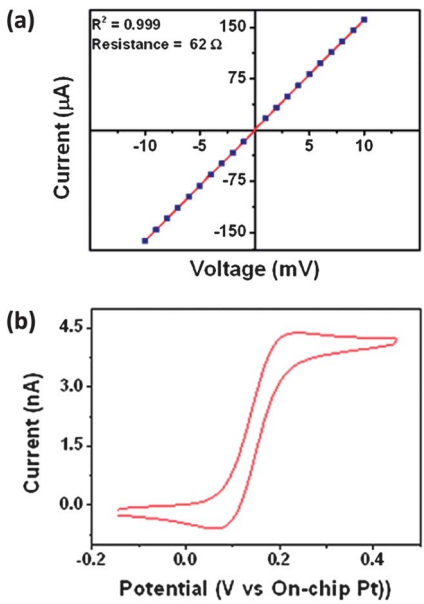

Fig. 2 Typical two point *I–V* characteristics measured for nanowire arrays comprising of four nanowires exhibit Ohmic behaviour and low contact resistances. Average resistance is 62 ± 4 Ω. (b) Typical voltammogram obtained for a nanowire array and in 1 mM FcCOOH in 10 mM PBS in the voltage range of −0.15 V to 0.45, pH 7.4.

Cyclic voltammetry (CV) is conducted in 10 mM phosphate buffer saline (PBS, pH 7.4) containing 1 mM FcCOOH in the voltage range of −0.15 V to 0.45, *versus* the on-chip platinum pseudo-reference. Fig. 2(b) shows a typical CV for FcCOOH recorded at 100 mV s^{-1}. CVs exhibit semi-infinite diffusive behaviour and demonstrate that the silicon nitride passivation layer has been successfully removed to expose the underlying nanowire arrays. The magnitude of the current, typical of nanowire arrays, confirms that electrochemistry only occurs at the nanowire electrodes and the passivation layer successfully prevents unwanted electrochemistry occurring at on-chip metallisation. Nanowire devices that exhibited lower or no electrochemical current were discarded and not used for further experiments.

The electrochemical reduction and oxidation of the nitroaromatics, shown in Scheme 1, are explored using cyclic voltammetry. Cyclic voltammograms of nitroaromatics are undertaken for 50 μg mL^{-1} concentrations of 3-NT, 2,4-DNT, 2,6-DNT, 1,3-DNB and TNT by scanning the voltage from 0 V to −1.0 V (reduction) followed by sweeping back to 0 V (oxidation) see Fig. 3. The measured peak from −0.6 V onwards may be attributed to the reduction of the phosphate buffer. No cathodic faradaic peaks are observed for any of the nitroaromatic molecules. A very small shoulder is evident on the TNT peak at −0.81 V *versus* the on-chip platinum pseudo-reference electrode. Very little hysteresis is evident on the CVs due to the inherent low capacitance of these nanowire electrode arrays. These results are in contrast to measurements reported using glassy carbon electrodes

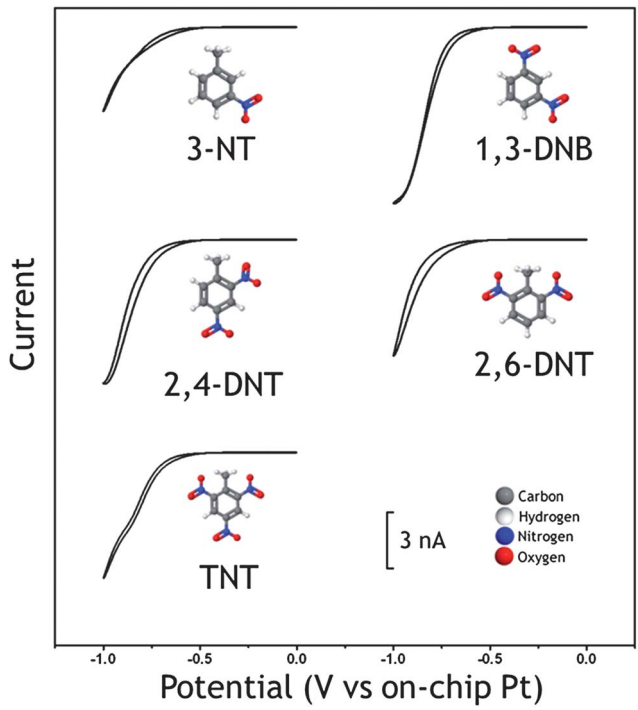

Fig. 3 Cyclic voltammograms recorded for five nitro aromatic species. The reductive peak above −0.6 V may be attributed to the reduction of the phosphate buffer.

which typically show clear reduction peaks and may be attributed to the low activity of gold towards the reduction of nitro groups.[27] Consequently CV is not a sensitive enough technique to maximise signal output.

By contrast, square wave voltammetry is a very sensitive electrochemical method, compared to cyclic voltammetry, which permits fast scan rates and is suitable for remote electroanalysis. Fig. 4 shows background subtracted square wave voltammograms for 50 μg mL^{-1} concentrations of 3-NT, 2,4-DNT, 2,6-DNT, 1,3-DNB and TNT in phosphate buffer undertaken using a nanowire array electrode comprising four nanowires and the following conditions: $E_{initial}$: −0.4V; E_{Final}: −1.02 V; amplitude: 50 mV; frequency 10 Hz; potential step: 4 mV. The reductive signals for the cathodic SWV show well defined peak potentials and are equalised to the 3-NT peak. The reduction of the nitro groups of TNT is characterised by a pair of reduction peaks at −671 mV and −882 mV, respectively. These peaks represent the reduction of the *ortho* nitro groups which are reduced at a lower potential due to their proximity to the electron donating methyl group at the 1 position.[26] The reduction of the *para* positioned nitro group is obscured possibly due to the sensitivity of our electrodes to reduction of the buffer at higher cathodic potentials. A single reduction peak is observed for 2,6-dinitrotoluene (−856 mV), 2,4-dinitrotoluene (−799 mV) and dinitrobenzene (−760 mV). It is again suspected that further expected peaks are obscured by the reduction of the phosphate buffer. A single peak is seen for 3-nitrotoluene at −900 mV. The higher cathodic potential needed for the reduction of 3-NT may be due to the position of the nitro group in relation to the methyl group. A methyl group in aromatic compounds is *ortho* and *para* directing due to resonance allowing the delocalisation of electrons around the aromatic ring, while reduction of the *meta* position nitro group in 3-NT is less favourable. From Fig. 4, it is evident that, due to the high sensitivity and low capacitance of the nanowires, the positions of reduction peaks are clearly resolved for the different molecules. This is exemplified by the ability to resolve the *ortho* reduction peaks of the two isomers 2,4-DNT and 2,6-DNT.

The ability to resolve clearly the position of the SWV cathodic potential peaks lends the data suitability for principle component analysis (PCA). PCA is an

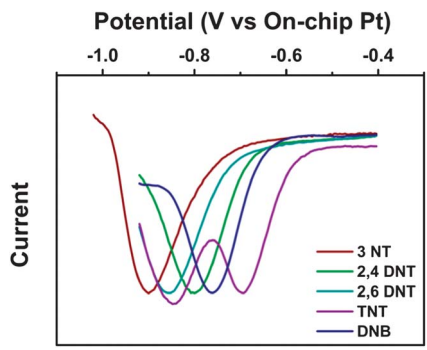

Fig. 4 Background subtracted square wave voltammograms for 50 μg mL^{-1} concentrations of 3-NT, 2,4-DNT, 2,6-DNT, 1,3-DNB and TNT in phosphate buffer pH 6.5, $E_{initial}$: −0.4V; E_{Final}: −1.02 V; amplitude: 50 mV; frequency 10 Hz; amplitude: 4 mV.

unsupervised method with no *prior* knowledge of experimental structure and is used to reduce the dimensionality of the data and explain the variance–covariance structure of a set of variables through a few linear combinations of these variables.[28] In PCA the linear combinations (PCs) of the original variables are orthogonal (uncorrelated) to each other and much of the original data variability can be accounted for by a small number of PCs which are then used for data dimensionality reduction and visual data interpretation. Before applying PCA, data needs to be adequately pre-processed and scaled. In this work, data is autoscaled so that the variable measured (peak potential) had a mean equal to zero and a standard deviation equal to one. Rows on the data matrix used for PCA represent nitro compounds tested using a unique column representing their respective measured peak potential values. The software package used for the PCA analysis was R version 2.9.2 (R: A Language and Environment for Statistical Computing, Vienna, Austria, 2009).

The first principal component scores (PC1) against a sample index to visualize the discrimination between compounds; see Fig. 5. As this data set is composed by only one variable, only one PC can be computed and PC1 explains 100% of the data variance. Each compound forms a clearly distinguishable cluster and all compounds are successfully discriminated by unsupervised cluster analysis; see Fig. 5. In addition, two different samples of the TNT compound were tested (one military grade and one analytical standard, represented by a diamond and a down triangle, respectively). The results show that the two different TNT samples also form unique clusters. As PCA is an unsupervised technique and does not know the identity (nitro compound class) of the samples, these results suggest that the devices successfully detected consistent similarities between readings of the same compound and consistent dissimilarities between readings of different compounds which, when translated into peak potential signals, enable accurate discrimination of nitro compounds.

Calibration curve for TNT

To demonstrate the suitability of the nanowire arrays as sensors for nitroaromatics, calibration experiments were undertaken to examine the effects of

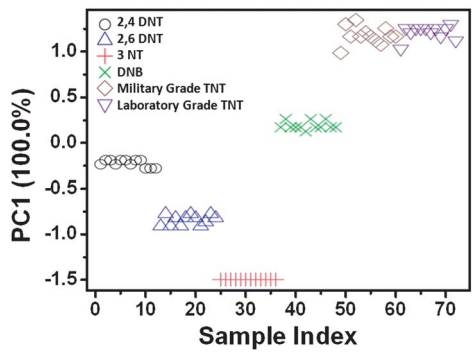

Fig. 5 Cluster analysis: scores plot from PCA applied to the data collected by the "8 (4 × 700 nm Band)" device. The data were autoscaled to previous PCA and as the dataset is composed by only 1 variable, the peak potential, PC1 explains 100% of the data variance.

increasing concentration on the SWV signals using a serial addition approach. Once recorded, the measurements are background-subtracted to give the distinct TNT peaks shown in Fig. 4.

Fig. 6 shows the calibration plot for military grade TNT. Each measurement was undertaken four times to monitor the stability and reproducibility of the electrodes and the error bars represent the standard deviation from the mean value. The limit of detection was sub-150 ng mL^{-1} and a coefficient of $R^2 = 0.996$ showing good linearity with increasing concentration in this concentration range. The reproducibility and selectivity of cathodic SWV is a useful analytical tool and clearly demonstrates the viability of this approach to the selective detection of nitroaromatic species. Work is now on-going to develop this approach further: to examine different mixtures of nitroaromatic species; to increase sensitivity further by increasing the number of nanowires within an array; and by development of an ionic liquid overlayer, selectively permeable to nitroaromatics, to prevent unwanted interference from other reductive species.

4 Conclusions

We show a photolithography technique that permits gold nanowire array electrodes to be fabricated routinely at reasonable cost. Nanowire electrode arrays offer the potential for enhancements in electroanalysis including: increased signal-to-noise ratio and increased sensitivity while also allowing quantitative detection at much lower concentrations. Characteristic reduction peaks of nitro groups were not observed at nanowire array electrodes using sweep voltammetric methods. By contrast, clear and well defined reduction peaks were resolved using potential step square wave voltammetry. Principle component analysis was employed to discriminate between nitroaromatic species, including structural isomers of DNT. Finally, the magnitude of the reduction peak at −671 mV for different concentrations of TNT exhibited very good linearity enabling limits of detection at concentrations sub-150 ng mL^{-1}.

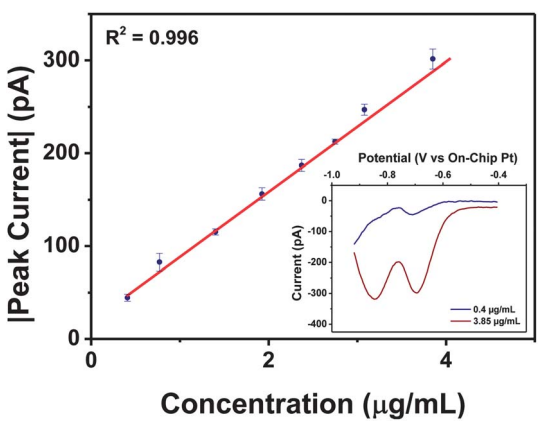

Fig. 6 Calibration plot of TNT obtained using peak currents measured at −671 mV. Inset: SWV voltammograms obtained for 0.40 and 3.8 μg mL^{-1}, respectively.

Acknowledgements

The authors gratefully appreciate assistance provided by the Ordnance School of Defence Forces, Ireland. This work was supported by Science Foundation Ireland under the Research Frontiers Programme (SFI/09/RFP/CAP2455), by the European Commission under the FP7 Security Project CommonSense (261809) and FP7 ICT project "Nanofunction" (257375) and the Irish Higher Education Authority PRTLI programs (Cycle 3 "Nanoscience" and Cycle 4 "INSPIRE").

Notes and references

1 M. Park, L. N. Cella, W. Chen, N. V. Myung and A. Mulchandani, *Biosens. Bioelectron.*, 2010, **26**, 1297–1301.
2 S. S. Talmage, D. M. Opresko, C. J. Maxwell, C. J. Welsh, F. M. Cretella, P. H. Reno and F. B. Daniel, *Rev. Environ. Contamination Toxicol.*, 1999, **161**, 1–156.
3 D. L. Kaplan and A. M. Kaplan, *Environ. Sci. Technol.*, 1982, **16**, 566–571.
4 W. D. Won, L. H. Disalvo and J. Ng, *Appl. Environ. Microbiol.*, 1976, **31**, 576–580.
5 W. C. C. Roberts, B. J. Commons, H. T. Bausum, C. O. Abernathy and J. J. Murphy, *U. S. Environmental Protection Agency*, 1993, EPA 822-R-93-022.
6 A. M. C. J. I. Jerez Rozo, S. L. Pena and S. P. Hernandez-Rivera, *Proc. SPIE–Int. Soc. Opt. Eng.*, 2007, **6538**, 653824.
7 C. A. Weisberg and M. L. Ellickson, *Am. Lab.*, 1998, **30**, 32N.
8 D. R. Shankaran, K. V. Gobi, T. Sakai, K. Matsumoto, T. Imato, K. Toko and N. Miura, *IEEE Sens. J.*, 2005, **5**, 616–621.
9 C. A. Heller, R. R. McBride and M. A. Ronning, *Anal. Chem.*, 1977, **49**, 2251–2253.
10 C. Keuchel, L. Weil and R. Niessner, *Anal. Sci.*, 1992, **8**, 9–12.
11 Gaurav, A. K. Malik and P. K. Rai, *J. Hazard. Mater.*, 2009, **172**, 1652–1658.
12 S. Babaee and A. Beiraghi, *Anal. Chim. Acta*, 2010, **662**, 9–13.
13 M. Agah, G. R. Lambertus, R. Sacks and K. Wise, *J. Microelectromech. Syst.*, 2006, **15**, 1371–1378.
14 Y. Cui, Z. H. Zhong, D. L. Wang, W. U. Wang and C. M. Lieber, *Nano Lett.*, 2003, **3**, 149–152.
15 C. Staii and A. T. Johnson, *Nano Lett.*, 2005, **5**, 1774–1778.
16 C. P. Chen, A. Ganguly, C. Y. Lu, T. Y. Chen, C. C. Kuo, R. S. Chen, W. H. Tu, W. B. Fischer, K. H. Chen and L. C. Chen, *Anal. Chem.*, 2011, **83**, 1938–1943.
17 C. M. Hangarter, M. Bangar, A. Mulchandani and N. V. Myung, *J. Mater. Chem.*, 2010, **20**, 3131–3140.
18 G. M. Cohen, M. J. Rooks, J. O. Chu, S. E. Laux, P. M. Solomon, J. A. Ott, R. J. Miller and W. Haensch, *Appl. Phys. Lett.*, 2007, **90**, 233110.
19 D. W. M. Arrigan, *Analyst*, 2004, **129**, 1157–1165.
20 K. Dawson, A. Wahl, R. Murphy and A. O'Riordan, *J. Phys. Chem. C*, 2012, **116**, 14665–14673.
21 K. Dawson, M. Baudequid, N. Sassiat, A. J. Quinn and A. O'Riordan, *Electrochim. Acta*, 2013, **101**, 169–176.
22 S. Guo, D. Wen, S. Dong and E. Wang, *Talanta*, 2009, **77**, 1510–1517.
23 K. Dawson, J. Strutwolf, K. P. Rodgers, G. Herzog, D. W. M Arrigan, A. J. Quinn and A. O'Riordan, *Anal. Chem.*, 2011, **83**, 5535–5540.
24 P. Tyagi, D. Postetter, D. L. Saragnese, C. L. Randall, M. A. Mirski and D. H. Gracias, *Anal. Chem.*, 2009, **81**, 9979–9984.
25 K. Dawson, M. Baudequin and A. O'Riordan, *Analyst*, 2011, **136**, 4507–4513.
26 C. K. Chua, M. Pumera and L. Rulisek, *J. Phys. Chem. C*, 2012, **116**, 4243–4251.
27 M. Galik, A. M. O'Mahony and J. Wang, *Electroanalysis*, 2011, **23**, 1193–1204.
28 R. A. Johnson and D. W. Wichern, *Applied Multivariate Statistical Analysis*, Prentice Hall, 2007.